www.czasopisma.pan.pl PAN www.journals.pan.pl
Chemical and Process Engineering 2018, 39 (2), 155–163
DOI: 10.24425/119106

THE INFLUENCE OF HYDRODYNAMIC CONDITIONS ON THE RECOVERY OF ACETONE, BUTANOL AND ETHANOL IN PERVAPORATION MEMBRANE MODULES

Joanna Marszałek*, Michał Tylman, Paulina Rdzanek, Władysław Kamiński

Lodz University of Technology, Faculty of Process and Environmental Engineering,
90-924 Lodz, Wolczanska 213, Poland

In order to assess the influence of hydrodynamic effects on the recovery of *n*-butanol by means of pervaporation, a commercial PERVAP 4060 membrane was investigated. Laboratory pervaporation experiments were carried out providing a comparison of the permeation fluxes and enrichment factors. While the enrichment factors achieved in both modules under the same process conditions were comparable, the permeation fluxes differed from each other. In order to explain the observed differences, hydrodynamic conditions in the membrane module were examined by means of CFD simulation performed with ANSYS Fluent 14.5 software. Two different modules having membrane diameters of 80 mm and 150 mm were analyzed. As a result, different velocity profiles were obtained, which served to estimate the mass transfer coefficients of butanol, ethanol and acetone.

Keywords: pervaporation, membrane module, flow modeling, biobutanol

1. INTRODUCTION

Pervaporation is a process for separating liquid mixtures with the help of solid non-porous membranes. Components of the feed solution transferred through the membrane are first adsorbed onto the membrane surface and dissolved, then diffuse across and are desorbed from the other side of the membrane. The efficiency of separation is influenced mainly by the interactions between the membrane and the feed solution as well as concentration polarization at the membrane/solution interface, resulting from the feed flow hydrodynamics. Within the boundary layer components are transferred by diffusion. Until mass transfer resistance of the layer is low enough, compared with diffusion resistance inside the membrane material, the boundary layer does not dominate the overall mass transfer. However, if the boundary layer resistance is high, it impedes the passage of molecules from the feed. In general, the thickness of the active layer governs pervaporation performance (Baig, 2008; Baker et al., 1997; Basile et al., 2015; George and Thomas, 2001).

Components of the feed solution diffuse through the polarization layer formed at the membrane surface. In the investigated system, mass is transferred from a quaternary feed containing acetone, butanol, ethanol and water. Acetone, butanol and ethanol are present in the ABE fermentation broth in a mass ratio of about 3 : 6 : 1 with the concentration of butanol typically lower than 3 wt%. Since purification of biobutanol carried out via distillation consumes a great amount of energy, other separation methods are being studied,

* Corresponding author, e-mail: joanna.marszalek@p.lodz.pl

including adsorption, gas stripping, perstraction, liquid-liquid extraction, pervaporation and reverse osmosis. Analysis of these methods leads to the conclusion that pervaporation is highly competitive because it allows simultaneous separation and enrichment of butanol with a hydrophobic membrane (Abdehagh et al., 2014; Huang et al., 2014; Liu et al., 2005).

It is commonly accepted in membrane science that scaling up from laboratory experiments to commercial production is not problematic, i.e. it is usually sufficient to increase the membrane area in order to proportionally raise the production rate. This notion, however, does not apply to flat membranes, which are susceptible to hydrodynamic properties of the system. For this reason, scaling up the process performed with a flat membrane should be preceded with fluid flow modeling in the membrane module.

This paper aims to assess the influence of the feed flow hydrodynamics on the pervaporative recovery of butanol. In order to achieve this goal, a commercial PERVAP 4060 membrane was investigated, placed in two membrane modules of different diameters. Hydrodynamic conditions in the modules were analyzed with the help of computational fluid dynamics (CFD) using ANSYS Fluent 14.5. Moreover, the achievable enrichment of butanol during pervaporation was studied experimentally.

2. EXPERIMENTAL METHODS

The experiments were performed using the laboratory equipment schematically shown in Fig. 1. The pervaporation system included two replaceable membrane modules designated for membranes 80 mm and 150 mm in diameter. The feed flow rate was equal to 40 dm^3/h. Figs. 3a and 4a present schematic cross-sections of the modules together with their internal dimensions. As the feed, an aqueous solution was used, containing acetone, *n*-butanol and ethanol in a 3 : 6 : 1 mass ratio. The feed was meant to imitate the ABE fermentation broth (Marszałek and Kamiński, 2012).

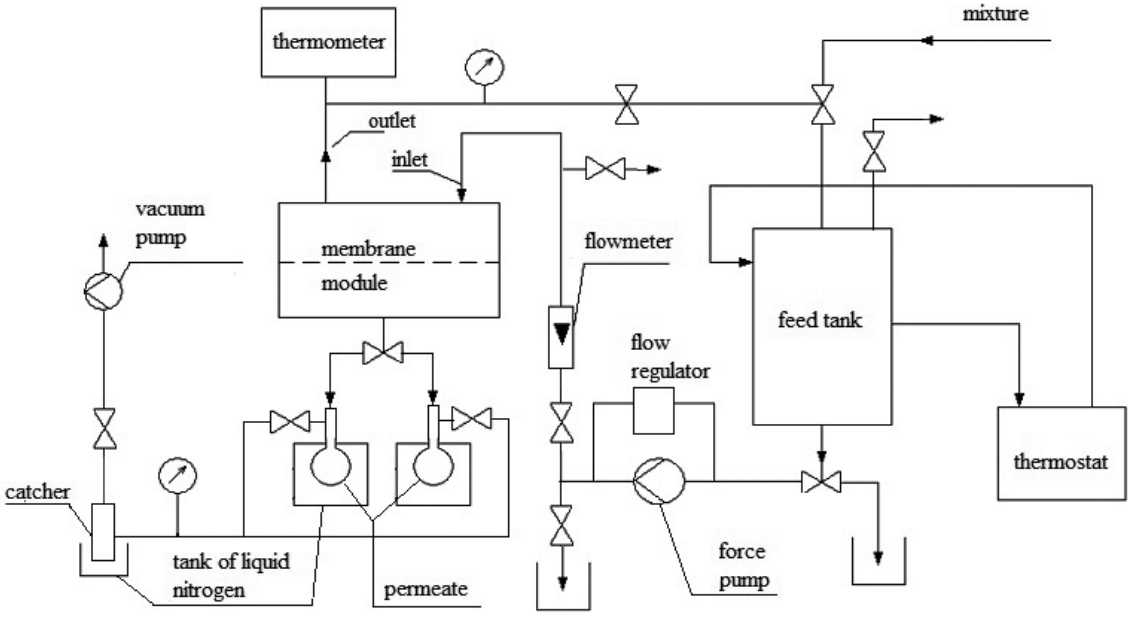

Fig. 1. Schematic diagram of the laboratory pervaporation system

2.1. Recovery of butanol in the pervaporation process

To examine the pervaporative recovery of butanol, a commercial hydrophobic PERVAP 4060 membrane was used, 80 mm and 150 mm in diameter, placed in the corresponding membrane modules. The process

was carried out at 29, 37 and 50 °C. The pressure on the low-pressure side of the membrane was constant and equal to 1 kPa. The feed contained 1.5, 3.0 or 5.0 wt% *n*-butanol, 0.75, 1.5 or 2.5 wt% acetone and 0.25, 0.5 or 0.83 wt% ethanol, respectively.

Samples of the feed, the permeate and the retentate collected during the process were analyzed using a ThermoFinnigan gas chromatograph equipped with a BTR-CW column and a 5 wt% solution of methanol in water as the internal standard (Marszałek and Kamiński, 2012).

3. RESULTS AND DISCUSSION

3.1. Pervaporation performance in the membrane modules

To investigate the recovery of butanol in the pervaporation process, laboratory experiments were carried out with two membrane modules 80 mm and 150 mm in diameter. Pervaporation performance is most often described using the flux of the permeating component and its enrichment factor obtained with a given membrane. In this work, these quantities, given by Eqs. (1) and (2), were used to determine the pervaporative separation of acetone, butanol and ethanol from aqueous feed solutions.

$$J_i = J_{tot}\, w_{iP} \tag{1}$$

$$\beta_i = \frac{w_{iP}}{w_{iF}} \tag{2}$$

The experimental values of permeation fluxes of acetone, butanol and ethanol in both investigated membrane modules, recorded at different feed concentrations of acetone, butanol and ethanol and different temperatures are shown in Figs. 2a and 2b. The enrichment factors achieved using different initial feed compositions are given in Table 1.

Table 1. Acetone, butanol and ethanol enrichment factors, β_i, achieved in both membrane modules

$w_{BuOH,F}$	80 mm module			150 mm module		
$[10^{-2}$g/g]	β_{Acet}	β_{BuOH}	β_{EtOH}	β_{Acet}	β_{BuOH}	β_{EtOH}
1.5	34.45	16.59	2.80	29.83	16.90	2.75
3	20.75	13.73	3.84	20.97	10.57	3.09
5	14.91	8.57	3.09	14.37	9.59	2.70

During the process performed in the smaller module, higher total and partial permeation fluxes of acetone, butanol and ethanol were observed in comparison with the larger module. The differences between the fluxes grew proportionally to the process temperature, reaching over a two-fold increase at 50 °C and 5 wt% butanol in the feed.

The efficiency of separation in the pervaporation process can also be measured with the enrichment factor defined as the concentration of a component in the permeate relative to its concentration in the feed solution. Table 1 compares the enrichment factors achieved using different compositions of the feed at 37 °C. As can be seen from the table, both membrane modules allow attaining similar enrichment factors when the same compositions of the feed solution are used. Also, acetone is separated most efficiently, followed by butanol and then ethanol.

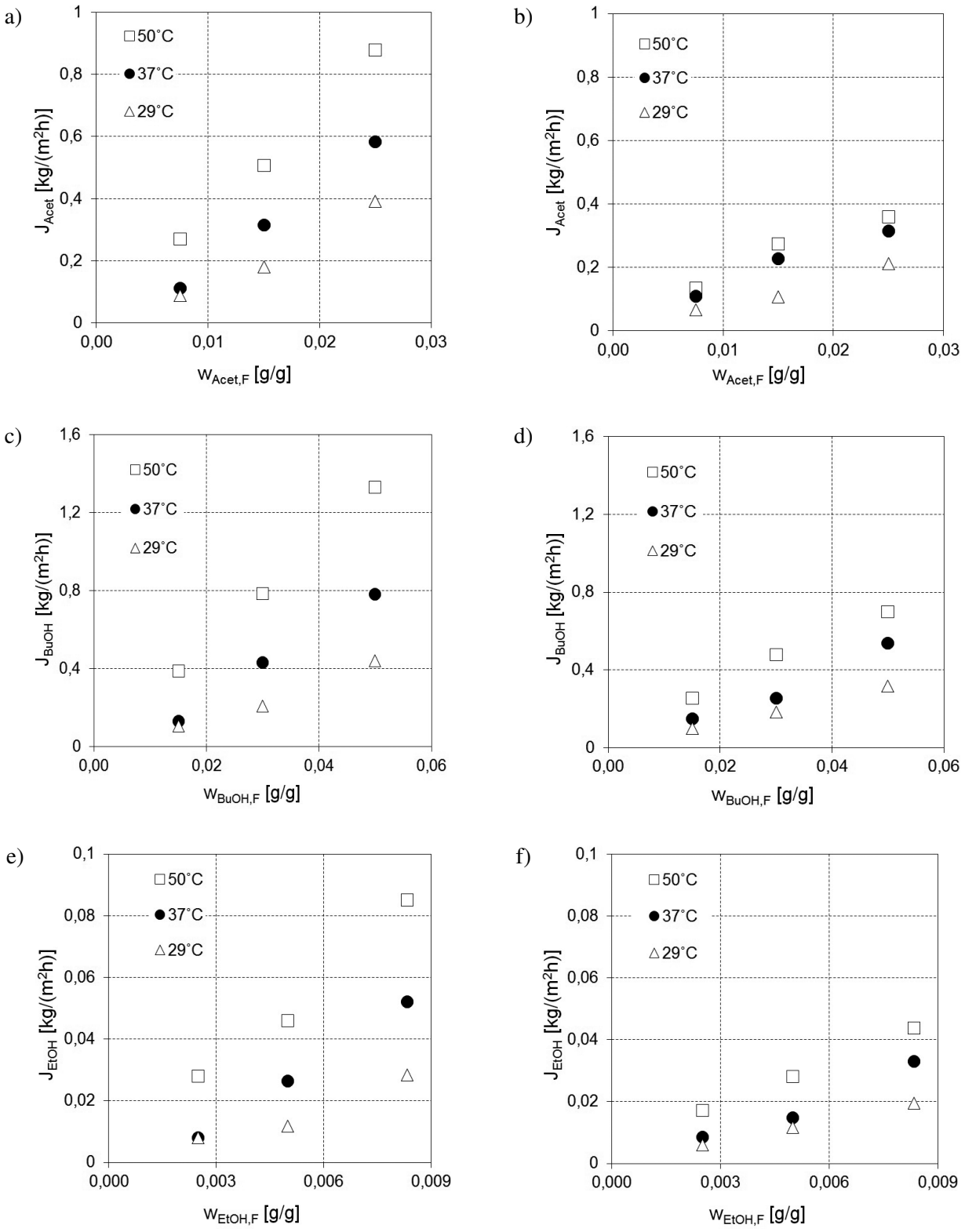

Fig. 2. Permeation fluxes of acetone, butanol and ethanol, J_{Acet}, J_{BuOH}, J_{EtOH} vs. concentrations of acetone, butanol and ethanol in the feed, $w_{Acet,F}$, $w_{BuOH,F}$, $w_{EtOH,F}$ in the membrane module a), c), e) 80 mm in diameter; b), d), f) 150 mm in diameter

The resulting permeate composition is influenced mainly by the membrane itself, but also by the process parameters (such as temperature) affecting the rate of diffusion through the membrane. For this reason, increasing the size of the membrane does not change the attainable enrichment factors in a significant manner, which has been corroborated by the experimental results.

In order to explain why the smaller module provided higher total and partial permeation fluxes of acetone, butanol and ethanol in comparison with the larger module, numerical simulations of the feed flow were undertaken. Afterwards, on the basis of the flow profiles and physicochemical properties of the fluid, the mass transfer coefficients were assessed, which was the main task of this paper.

3.2. Numerical simulation of feed flow in the membrane modules

According to numerous scientific reports, Computational Fluid Dynamics (CFD) is often used as an engineering tool to characterize hydrodynamics of fluid flow (Krawczyk et al., 2012; Moraveji et al. 2013; Schafer and Crespo, 2007).

In this work, Ansys Fluent 14.5 was employed to model the feed flow through two different membrane modules. The calculation range covered the inlet and the interior of the module. The simulations were performed using ANSYS Fluent 14.5 software. The calculation domain in the 80 mm module contained 19495 mesh elements and 10664 nodes. The maximum size of a triangular mesh element was 1.2×10^{-3} m. In the 150 mm module, these parameters were as follows: 55922 mesh elements, 108736 nodes, the maximum element size 1.2×10^{-3} m. For simulation purposes, temperatures of 29, 37 and 50 °C were assumed along with the physicochemical properties of the fluid corresponding to 1.5, 3.0 and 5.0 wt% *n*-butanol in the feed solution.

Figures 3 and 4 present the simulated velocities of the fluid in both modules i.e. the 80 mm module (Fig. 3a) and 150 mm module (Fig. 4a) at a temperature of 29 °C and a concentration of butanol in the feed equal to 3 wt%. Figs. 3b and 4b show velocity profiles at three selected cross-sections of each membrane module, located at a distance of 0.25, 0.5 and 0.75 of the membrane radius from the axis of the feed inlet.

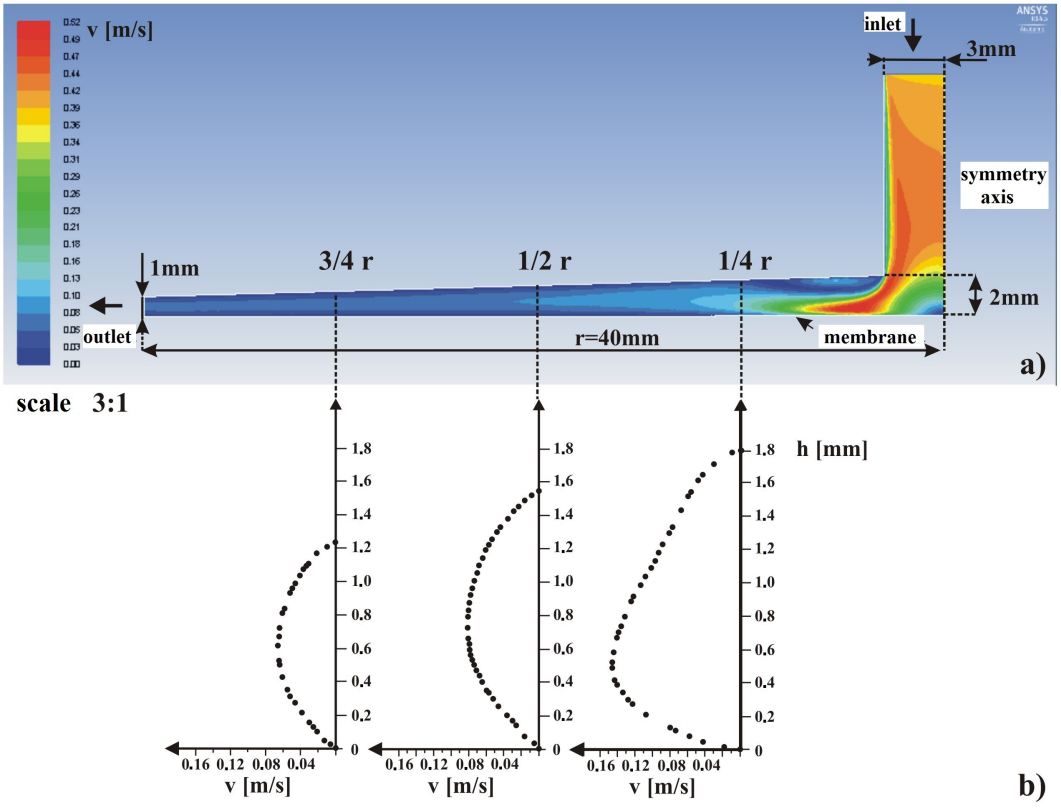

Fig. 3. a) Numerical simulation of the local feed velocities (m/s) over the membrane inside the 80 mm membrane module; b) Velocity profiles at selected cross-sections of the module

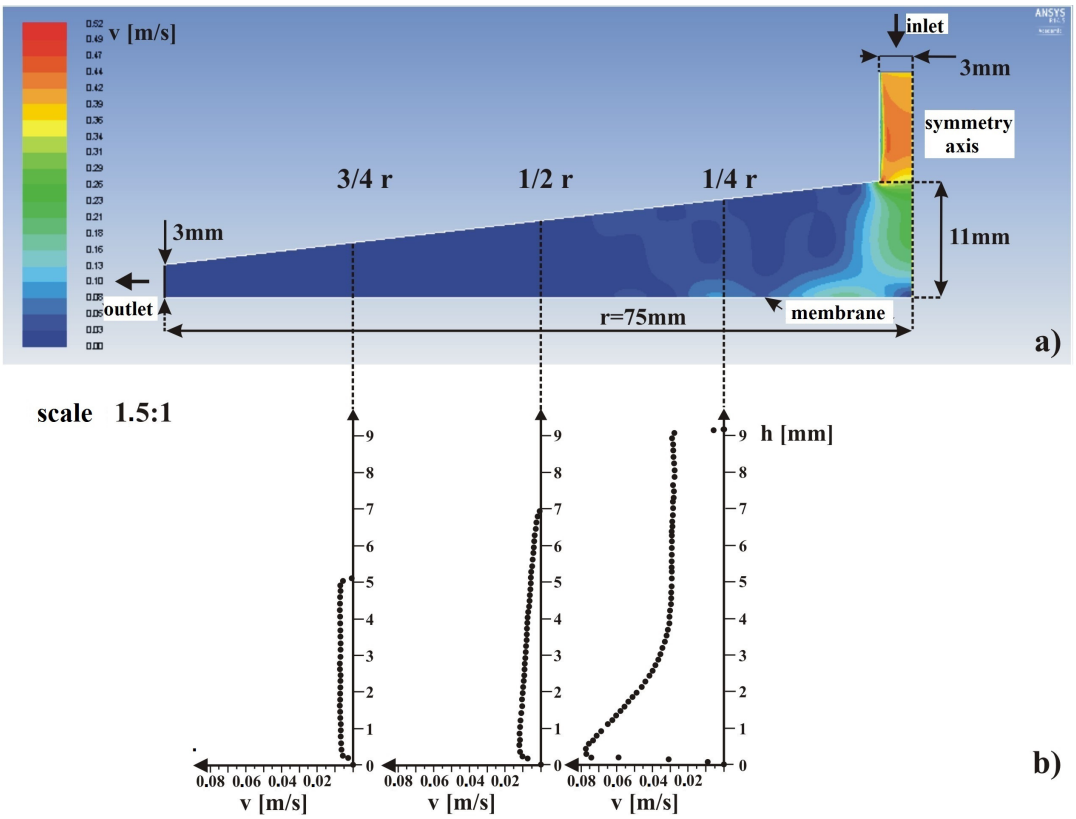

Fig. 4. a) Numerical simulation of the local feed velocities (m/s) over the membrane inside the 150 mm membrane module; b) Velocity profiles at selected cross-sections of the module

Local velocity profiles in the respective modules differ from each other because of the differences in their size and shape. Both modules are cone-shaped with their tops cut off where the feed inlets having a diameter of 6 mm had been attached. The distances between the membrane and the inner upper wall of the module at the inlet are 2 mm in the smaller and 11 mm in the larger module, which is illustrated in Figs. 2a and 3a. The analogous distances at the bottom of the module (at the outlet) are 1.0 mm and 3.0 mm, respectively.

At the feed inlet, certain disturbances can be observed resulting from its geometry. At the membrane surface, the velocity profiles differ depending on the distance from the inlet axis. Considering the size of both modules and their geometry and with the help of the simulation results, the mean velocity of the fluid has been determined. At a distance of one fourth of the membrane radius from the inlet axis (10 mm in the smaller and 18.75 mm in the larger module), the mean flow velocity is equal to 0.093 m/s and 0.0365 m/s, respectively. The mean velocities at distances of 0.5 and 0.75 of the membrane radius from the inlet are presented in Tables 2 and 3.

Table 2. Distances for the 80 mm module cross sections and mass transfer coefficients

x	x	u_{ax}	k_{Acet}	k_{BuOH}	k_{EtOH}
[–]	[mm]	[m/s]	[10^{-5} m/s]	[10^{-5} m/s]	[10^{-5} m/s]
0.25r	10.00	0.0930	2.47	2.04	2.40
0.5r	20.00	0.0550	1.34	1.11	1.31
0.75r	30.00	0.0453	1.00	0.82	0.97

Table 3. Distances for the 150 mm module cross sections and mass transfer coefficients

x	x	u_{ax}	k_{Acet}	k_{BuOH}	k_{EtOH}
[–]	[mm]	[m/s]	[10^{-5} m/s]	[10^{-5} m/s]	[10^{-5} m/s]
0.25r	18.75	0.0365	1.13	0.93	1.10
0.5r	37.50	0.0066	0.34	0.280	0.33
0.75r	56.25	0.0058	0.260	0.22	0.25

The general approach to predicting mass fluxes in pervaporation has been presented by Kubaczka et al. (2018). It is very complicated mathematically and beyond the scope of this paper. However, to explain why the total and partial permeation fluxes of acetone, butanol and ethanol were higher in the smaller module, we decided to calculate the mass transfer coefficients. The correlation given by Eq. (3) (Rousseau, 1987) was assumed appropriate for the flow over a flat surface. The permeation flux depends on the mass transfer resistance in the flow near the surface of the membrane and diffusive resistance within the membrane. Since the same membrane was used in all experiments, the differences in mass transfer in the feed flow resulted in the permeation flux differences.

$$Sh = 0.664\, Re^{0.5} Sc^{0.33} \tag{3}$$

$$k_i = \frac{Sh_i D_{wi}}{x} \tag{4}$$

where Re is the Reynolds number defined as:

$$Re_x = \frac{u_{ax}\, x\, \rho_F}{\mu_F} \tag{5}$$

where u_{ax} – average velocity of the fluid at an x cross section of the module.

The results of calculations that were performed for a temperature of 29 °C are summarized in Table 2 for the 80 mm module and Table 3 for the 150 mm module. The calculated Reynolds number increases from 1136 to 1660 in the small module along with the distance from the inlet and decreases from 836 to 398 in the large module. Its values suggest laminar flows in both modules.

The diffusivity necessary for calculating the Schmidt number were taken from Hills et al. (2011). Taking into account that the aqueous solutions were diluted, their viscosity was assumed to be equal to the viscosity of water. The resulting Schmidt number was 639 for acetone, 852 for butanol and 665 for ethanol.

The mass transfer coefficients were calculated using the physicochemical properties of the components. However, it should be noted that their accuracy is about 20%.

Tables 2 and 3 show that the mass transfer coefficients of acetone, butanol and ethanol are several times higher for the 80 mm module compared to the 150 mm module. This is due to the higher linear flow rates and smaller distances between the feed inlet and the outlet.

4. CONCLUSIONS

- Experiments were carried out on the pervaporative concentration of diluted aqueous solutions of acetone, butanol and ethanol using flat membranes and two membrane modules 80 mm and 150 mm in diameter. Significant differences in the permeation fluxes were found when comparing the modules. On the other hand, the enrichment coefficients, determined by the membrane type, had similar values.

- Simulations of fluid flow through the two flat membrane modules show that the local velocity profiles in the modules differ from each other, which significantly influences the mass transfer coefficients and consequently the permeation of the feed components through the membrane.
- Considering the dimensions of flat modules, pervaporation studies should always be preceded by hydrodynamic analysis. Otherwise, it is not possible to adequately compare the results coming from different data sources.

SYMBOLS

D	diffusion coefficient of a component in water, m^2/s
h	module height, m
J	permeation flux, $kg/(m^2h)$
k	mass transfer coefficient, m/s
r	membrane radius measured from the axis of the feed inlet, m
Re	the Reynolds number
Sc	the Schmidt number
Sh	the Sherwood number
w	mass fraction of a component
u	flow velocity of the fluid, m/s
x	length of the flat plate, m

Greek symbols

β	enrichment factor
ρ	density of the fluid, kg/m^3
μ	viscosity of the fluid, Pa·s
φ	diameter of the module, mm

Subscripts

F	feed
i	number of component
P	permeate
w	water
x	selected cross-section of the membrane module
ax	average velocity of the fluid
tot	total
Acet	acetone
BuOH	butanol
EtOH	ethanol

REFERENCES

Abdehagh N., Tezel F.H., Thibault J., 2014. Separation techniques in butanol production: Challenges and developments. *Biomass bioenerg.*, 60, 222–246. DOI: 10.1515/cpe-2017-0008.

Baig F.U., 2008. Pervaporation, In: Li N.N., Fane A.G., Ho W.S.W., Matsuura T. (Eds.), *Advanced membrane technology and applications*, John Wiley & Sons, Inc., 469–488. DOI: 10.1002/9780470276280.ch17.

Baker R.W., Wijmans J.G., Athayde, A.L., Daniels, R., Ly, J.H., Le, M., 1997. The effect of concentarion polarization on the separation of volatile organic compounds from water by pervaporation. *J. Membr. Sci.*, 137, 159–172. DOI: 10.1016/S0376-7388(97)00189-0.

Basile A. Figoli A. Khayet M., 2015. *Pervaporation, vapour permeation and membrane distillation*, 1st edition, Woodhead Publishing.

George S.C., Thomas, S., 2001. Transport phenomena through polymeric systems. *Prog. Polym. Sci.*, 26, 985–1017. PII: S0079-6700700)00036-8. DOI: 10.1016/S0079-6700(00)00036-8.

Hills E., Abraham M.H., Hersey A., Beval C.D., 2011. Diffusion coefficients in ethanol and water at 298 K: Linear free energy relationships. *Fluid Phase Equilib.*, 303, 45–55. DOI: 10.1016/j.fluid.2011.01.002.

Huang H.-J., Ramaswamy S., Liu Y., 2014. Separation and purification of biobutanol during bioconversion of biomass. *Sep. Pur. Techn.*, 132, 513–540. DOI: 10.1016/j.seppur.2014.06.013.

Krawczyk M., Kaminski K., Petera J., 2012. Experimental and numerical investigation of electrostatic spray liquid-liquid extraction with ionic liquids*Chem. Process Eng.*, 33, 167–183. DOI: 10.2478/v10176-012-0015-0.

Kubaczka A., Kaminski W., Marszalek J., 2018. Predicting mass fluxes in the pervaporation process using Maxwell–Stefan diffusion coefficients. *J. Mem. Sci.*, 546, 11–119. DOI: 10.1016/j.memsci.2017.08.074.

Liu F., Liu L., Feng X., 2005. Separation of acetone-butanol-ethanol (ABE) from dilute aqueous solution by pervaporation. *Sep. Pur. Techn.*, 42, 273–282. DOI: 10.1016/j.seppur.2004.08.005.

Marszałek J., Kamiński W., 2012. Efficiency of acetone-butanol-ethanol-water system separation by pervaporation. *Chem. Process Eng.*, 33, 131–140. DOI: 10.2478/v10176-012-0012-3.

Moraveji M.K., Raisi A., Hosseini S.M., Esmaeeli E., Pazuki G., 2013. CFD modelling of hydrophobic pervaporation process: ethanol/water separation. *Desalin. Water Treat.*, 51, 16–18, 3445–3453. DOI: 10.1080/19443994.2012.749325.

Rousseau R.W., 1987. *Handbook of separation process technology*. John Wiley & Sons.

Schafer T., Crespo J.G., 2007. Study and optimization of hydrodynamic upstream conditions during recovery of a complex aroma profile by pervaporation. *J. Membr. Sci.*, 301, 46–56. DOI: 10.1016/j.memsci.2007.05.034.

Received 12 July 2017
Received in revised form 20 April 2018
Accepted 25 April 2018